

Quantitative crystal structure descriptors from multiplicative congruential generators

Wolfgang Hornfeck

Received 12 June 2011
Accepted 21 November 2011

Institut für Materialphysik im Weltraum, Deutsches Zentrum für Luft- und Raumfahrt (DLR), Linder Höhe, D-51147 Köln, Germany. Correspondence e-mail: wolfgang.hornfeck@web.de

Special types of number-theoretic relations, termed multiplicative congruential generators (MCGs), exhibit an intrinsic sublattice structure. This has considerable implications within the crystallographic realm, namely for the coordinate description of crystal structures for which MCGs allow for a concise way of encoding the numerical structural information. Thus, a conceptual framework is established, with some focus on layered superstructures, which proposes the use of MCGs as a tool for the quantitative description of crystal structures. The multiplicative congruential method eventually affords an algorithmic generation of three-dimensional crystal structures with a near-uniform distribution of atoms, whereas a linearization procedure facilitates their combinatorial enumeration and classification. The outlook for homometric structures and dual-space crystallography is given. Some generalizations and extensions are formulated in addition, revealing the connections of MCGs with geometric algebra, discrete dynamical systems (iterative maps), as well as certain quasicrystal approximants.

© 2012 International Union of Crystallography
Printed in Singapore – all rights reserved

1. Introduction

As the Pythagoreans would have put it: all is number.

Among many other things, the geometers of ancient Greece put a particular emphasis on the *proportions* between numbers, rather than regarding them as singular entities, which ultimately led them to the discovery of incommensurate measures of irrational length ratio.

The scope of this work is to convey the idea of proportion from number theory into crystallography.

Whereas the geometrical notion of (in)commensurate measures is already well established among crystallographers, the number-theoretic one, originating from the fundamental relation of modular arithmetics, *i.e.* the congruence

$$y \equiv mx \pmod{M}, \quad (1)$$

seems to be far less explored. We argue that the integers m and M can be interpreted as two independent scales of spatial extension, *i.e.* translational periods, and that there lies some advantage in doing so. The successive operations of multiplication and division with a remainder, *i.e.* up-scaling and down-projecting, define a mapping between a pair (x, y) of coordinates, which, upon iteration, entails a cyclic behaviour – that of a *multiplicative congruential generator* (MCG).

Applied to the coordinate description of crystal structures, this observation sheds light on rather subtle interrelations between a crystal structure's atomic coordinates – in some way matching the symmetry of the spatial arrangement of atoms, in some other ways extending it – which may be employed to

compactify its numerical representation, therefore yielding what we call a *quantitative crystal structure descriptor* (QCSD).

1.1. General remarks

The following paragraphs give a comprehensive survey of MCGs, their sublattice structure and cycle representation. The presentation is restricted to features deemed essential for an understanding of the remainder of this paper, which covers a variety of distinct topics related to MCGs. For a detailed account of MCGs and their applications in crystallography see Hornfeck & Harbrecht (2009).

Comparatively novel concepts are preferably introduced by means of simple, well chosen examples. Hence, the previous analysis of MCGs was intentionally restricted to the special case of *planar similar* sublattices of *hexagonal* and *square* symmetry, which is generalized and extended in Appendix A. Some general mathematical properties of similar sublattices of planar lattices are described by Baake *et al.* (2011). Many of the introductory statements are mentioned here for the first time, tailored to clarify the previous knowledge, with an emphasis on a somewhat intuitive understanding of the fundamental ideas.

1.2. Multiplicative congruential generators

An MCG is defined by the recurrence relation

$$Z_{n+1} \equiv mZ_n \pmod{M} \quad (2)$$

where $m, M \in \mathbb{Z}$, with $M > m > 0$, and $Z_i \in \mathbb{Z}/M\mathbb{Z}$. The set $\mathbb{Z}/M\mathbb{Z} = \{0, 1, \dots, M-1\}$ is known as the residue class ring

to the modulus M . The integers m and M are called the multiplier and the modulus of an MCG, respectively. Other symbols may be used in order to emphasize special multipliers (e.g. μ or $\bar{\mu}$) or special moduli (e.g. T or Q). A given MCG describes a one-to-one mapping of the set $\mathbb{Z}/M\mathbb{Z}$ onto itself and thus is a *permutation* which may be represented in different ways. Take, for example, the MCG with $m = 3$ and $M = 7$ which results in the mapping of the set $\{0, 1, 2, 3, 4, 5, 6\}$ onto itself. The permutation may be represented either in two-line matrix notation

$$\begin{pmatrix} 0 & 1 & 2 & 3 & 4 & 5 & 6 \\ 0 & 3 & 6 & 2 & 5 & 1 & 4 \end{pmatrix}, \quad (3)$$

or as the *tuple* $(0, 3, 6, 2, 5, 1, 4)$, or as a decomposition into a product of disjoint *cycles*

$$(0)(1\ 3\ 2\ 6\ 4\ 5), \quad (4)$$

of length $\ell = 1$ and $\ell = 6$, respectively, or *via* the permutation matrix

$$\mathbf{P}(3, 7) = \begin{pmatrix} 1 & 0 & 0 & 0 & 0 & 0 & 0 \\ 0 & 0 & 0 & 1 & 0 & 0 & 0 \\ 0 & 0 & 0 & 0 & 0 & 0 & 1 \\ 0 & 0 & 1 & 0 & 0 & 0 & 0 \\ 0 & 0 & 0 & 0 & 0 & 1 & 0 \\ 0 & 1 & 0 & 0 & 0 & 0 & 0 \\ 0 & 0 & 0 & 0 & 1 & 0 & 0 \end{pmatrix} \Leftrightarrow \begin{pmatrix} \bullet & \circ & \circ & \circ & \circ & \circ & \circ \\ \circ & \circ & \circ & \bullet & \circ & \circ & \circ \\ \circ & \circ & \circ & \circ & \circ & \circ & \bullet \\ \circ & \circ & \bullet & \circ & \circ & \circ & \circ \\ \circ & \circ & \circ & \circ & \circ & \bullet & \circ \\ \circ & \bullet & \circ & \circ & \circ & \circ & \circ \\ \circ & \circ & \circ & \circ & \bullet & \circ & \circ \end{pmatrix}. \quad (5)$$

While the cycle notation of a permutation has the advantage of being concise, its matrix representation exhibits an otherwise hidden pattern, which is even more impressive when one makes the graphical substitutions $0 \rightarrow \circ$ and $1 \rightarrow \bullet$. One can clearly discern a regular, grid-like pattern, which reveals the *sublattice structure* of an MCG.

1.3. Sublattice structure of MCGs

The sublattice structure is also apparent when one is transforming the cycle representation of equation (4) to the point set

$$p(3, 7) = \left\{ (0, 0), \left(\frac{1}{7}, \frac{3}{7}\right), \left(\frac{3}{7}, \frac{2}{7}\right), \dots, \left(\frac{5}{7}, \frac{1}{7}\right) \right\} \quad (6)$$

by making a pairwise and circular overlapping combination of successive cycle elements with a subsequent division by the modulus M in order to obtain fractional coordinates. Drawn inside the frame of a symmetry-adapted unit cell relates this special MCG to the lattice–sublattice transformation of a hexagonal basic lattice to one of its similar sublattices of index 7 (Fig. 1, left). The successive shift in the (x, y) coordinates, encoded in the MCG, is equivalent to a discrete, periodic movement on the surface of a torus, constructed from the sublattice unit cell by gluing together pairs of parallel edges preserving their orientation, *i.e.* imposing periodic boundary conditions (Fig. 1, right).

1.4. Cycle representation of MCGs

Any MCG has its corresponding cycle representation, of which

$$(Z_{i1}Z_{i2} \dots Z_{i\ell_i})_{i=1}^n \quad (7)$$

is a general notation [with ℓ_i the length of the i th cycle and n the total number of cycles; *cf.* equation (4) for a special case]. Its most important feature within a crystallographic context is due to a previously described one-to-one correspondence between number-theoretic and crystallographic notions: most importantly between the set of crystallographic orbits, associated with a lattice–sublattice transformation of given index M , and a cycle representation, as induced by the action of an MCG with modulus M . In particular, the decomposition into a product of disjoint cycles resembles the splitting of sublattice sites into a set of crystallographic orbits (Hornfeck & Harbrecht, 2009), with the MCG-induced permutation of lattice-point coordinates preserving the point-group symmetry of the planar lattice.

2. Conceptual framework

A generally accepted definition of what should be regarded as a QCS is missing and its derivation appears to be a non-trivial task as well.

In our opinion, a *structural descriptor* is the result of logical reasoning according to some previously defined scheme or algorithm and applied to a given molecular or crystal structure, which covers some essential chemical facts about it. The

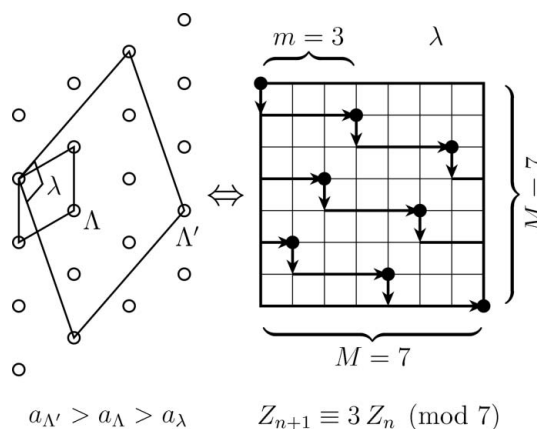


Figure 1 Sublattice structure of MCGs. Left: a lattice Λ (here a hexagonal one) with lattice parameter a_Λ and a like-oriented sub- and superlattice pair, Λ' and λ , for which $a_{\Lambda'} > a_\Lambda > a_\lambda$, such that the unit mesh areas A_i are in the ratio $A_{\Lambda'} : A_\Lambda : A_\lambda = M : 1 : M^{-1}$, where M is the sublattice index. Right: orthonormal redrawing of the superlattice λ , emphasizing the sequential generation of lattice points, by the action of an MCG with parameters m and M , according to the sublattice transformation $\Lambda \rightarrow \Lambda'$. Note that there is a sublattice structure for any choice of m and M (with respect to their admissible values; *cf.* §1.2), but that not every sublattice is primitive nor can it be embedded, under affine transformations of λ , as a (similar) sublattice of high, *i.e.* hexagonal or square, symmetry. The alternate movements along the two basic vectors of Λ' define a shift vector σ , which in the present case is given as $\sigma = (1/7, 3/7)_{\Lambda'}^t = (0, 1)_{\Lambda}^t = (1, 3)_{\lambda}^t$ in its respective reference frames.

vagueness of this definition allows one to summarize a great number of distinct concepts around the general idea of encoding structural information in some type of cipher, which in succession represents a suitable way to store, analyse or communicate the essential qualitative and quantitative features of a structure without referring to all of its details.

In the following we illustrate the rationale behind the suggested use of MCGs as QCSDs, putting a special emphasis on the principles and practice of finding suitable structural candidates.

2.1. Crystal structure descriptors

We choose to follow two complementary strategies:

(i) to review some basic ideas about structural descriptors employing concepts originally arising from *molecular* chemistry, and

(ii) to mention those *crystal* structure descriptors already established, but distinct from the ones we imagine and propose.

Everything is somewhat easier for molecules. Arguably the simplest structure descriptor of a molecule is its sum formula, encoding the information about the *arithmetical* proportions in which elements combine, *i.e.* a molecule's composition. On the next level, the structural formula of a molecule describes the mutual *topological* connection of atoms in a molecule, *i.e.* its constitution. At yet another level the *geometrical* arrangement of a molecule's atoms in space is accounted for, *i.e.* their configuration and conformation (Kerber *et al.*, 2004). From this it is clear that there exists a hierarchy of structural representations, differing in their respective information content, partially continuing to even higher levels of representations, as is the case for proteins where the linear sequence of amino acids subsequently determines its primary, secondary and tertiary structure. At every level of representation there may exist distinct types of structural descriptors. However, most of them are *qualitative* in nature, which suffices for most 'null-dimensional' molecules but certainly not for three-dimensional crystals.

For crystals, physical entities like the packing fraction or the number of formula units in a unit cell may act as a QCSD, and indeed are used for this purpose, sometimes extended by qualitative information like in the Pearson symbol. Interesting in their own right are topological descriptors, either as the topological indices of chemical graph theory derived from the scaffold of molecular structures (*e.g.* the famous Wiener index; Wiener, 1947), or as geometrical descriptors derived from the quotient graphs of crystal structures (*e.g.* Eon, 2011 and references therein). However, the calculation of atomic coordinates from these descriptors seems to be a tedious task, or the descriptor is defined the opposite way around, *i.e.* it is itself the result of a calculation based on the set of atomic positions. We also exclude any QCSD from the discussion that is based on classical concepts of crystallography and structural chemistry (see Burzlaff & Rothammel, 1992; Burzlaff & Malinovsky, 1997 for a survey), such as coordination numbers, the associated polyhedra or their duals, the Voronoï poly-

hedra, not because they are not useful in general (Mackay, 1984), *but* because they are not useful in general, for several reasons (Hoppe, 1998, 2004).

Essentially, we confine our argument to three widely used crystallo-chemical notations, which, in one aspect or another, convey our idea of what a structural descriptor should look like, except for their qualitative or semi-quantitative nature:

(i) Niggli's notation (*e.g.* ${}_{\infty}^2[\text{CC}_{3/3}]$ for the graphite structure) allows for a description of *mutual atomic coordination motifs* and gives further information about the predominant periodicity of partial structures. In the case of rather simple structures this information may be sufficient to reconstruct the shape of the coordination polyhedra and possibly the entire crystal structure.

(ii) Jagodzinski's notation (*e.g.* *hhc* for the structure of elemental Sm) is equally suitable when it comes to polytype structures and their stacking sequence. It is unique, owing to its construction from local information, *i.e.* the relative orientation of adjacent hexagonal closest-packed layers, and thus allows an *unambiguous reconstruction* of an albeit restricted class of structures.

(iii) Pearson's notation (*e.g.* *cF8* for the diamond structure) captures some essential crystallographic information, *i.e.* the crystal system, the Bravais type and the number of atoms in a unit cell, and proves to be especially useful in the classification of inorganic and intermetallic crystal structure types, although it is neither a unique descriptor nor does it contain any information about the mutual arrangement of atoms, despite its otherwise *quantitative* character.

An ideal QCSD should combine most of the aforementioned advantageous features such that it allows an unambiguous reconstruction of the structure, thus preserving the information about the mutual spatial arrangement of atoms.

2.2. MCGs as QCSDs

A crystal structure is usually described geometrically by giving its space-group symmetry, its unit-cell metric and the fractional coordinates of all atoms in an asymmetric unit. While this description is essentially complete, it is, however, cumbersome to evaluate or even to memorize, especially in the case of complex structures containing several hundreds of atoms in their unit cell. As it happens, the mandatory structural information is mostly missing in the original literature nowadays and electronic crystal structure databases, regardless of their advantage in general, are full of errors and omissions.

Would it not be nice if there was some way to store and memorize the crystallographic data, specifically the atomic coordinates, in a more comprehensive way? For example, by identifying some previously hidden relationships between them, even if these interconnections are not in strict conformity to space-group symmetry [symmetry is certainly one of the most powerful concepts in crystallography and science in general, but its alleged importance may likewise distract attention from local structural motifs and their pseudo-symmetry, as well as other subtle interrelationships (*e.g.*

metrical ones; see Janner, 2004 for an example), which may be much more important from a chemist's point of view]. Or, alternatively, to simultaneously approximate a given set of coordinate values to a certain precision (which may be quite low, *i.e.* of a magnitude similar to the experimentally determined standard deviations) by means of some mathematical function – comparatively less complex regarding the number of parameters to specify.

We argue that MCGs are such functions, encoding a wealth of geometric information with a very small number of parameters and, most notably, they are independent of the overall system size. This seems all the more true, since it was shown that iterative mappings are equivalent descriptions of MCGs and that iterative functions, quite similar to MCGs, exist which are capable of coding even such complex structures as quasi-crystal approximants by means of some recursive algorithm (*cf.* §A4).

2.3. Sublattice descriptions of layer structures

From the vast amount of literature on layer structures we outline a small selection of works, thereby exploring classes of crystal structures which may be alternatively described by means of the multiplicative congruential method. As a common feature, these works rely heavily on lattice–sublattice relationships, often including similar sublattices, in order to characterize the spatial arrangement of atoms and possibly vacancies of their constituent layers.

Subdivisions of the hexagonal net were devised by Loeb (1964) as examples in his modular approach regarding the systematic generation of crystal structures. The attribute *modular* has two meanings in this context: first, it describes the mere possibility of building complex structures out of simple units (*modules*), and second, it expresses the notion of what Loeb called a *modular algebra*, *i.e.* the existence of congruence relations between coordinates and their representation in the notation of *modular* arithmetics. In succession these relations were used by Loeb (1990; §6) to represent the invariant cubic lattice complexes *F*, *D* and *I* by means of distribution matrices, thereby anticipating the application of MCGs in crystallography (*cf.* Hornfeck & Harbrecht, 2009 for further references to the work of Loeb).

Similar sublattices of hexagonal and square symmetry appear again in the work of Takeda & Donnay (1965), now under the idiosyncratic term of *compound tessellations* introduced by Coxeter (1948). However, only a small number of actual representatives exhibiting a compound tessellation were described by them (*e.g.* the mineral klockmannite).

Pearson, on the other hand, devotes a whole chapter of his book (Pearson, 1972, §7) to structures based on the close packing of triangular close-packed nets and subdivisions thereof, thereby covering a variety of different structure types and stoichiometries. Pearson's approach in presenting a large compilation of crystal structures as derived from the complex stacking of like or distinct layers exhibits a high probability for the identification of possible candidates, for which the multi-

plicative congruential method should be applicable in one way or another.

Lattice subdivisions were furthermore emphasized by Iida (1957) studying the crystal structure of magnetic oxides, by Figueiredo (1973) systematically deriving the spatially homogeneous distribution of constituents within binary closest-packed layers of given composition, by Lima-de-Faria (1983) in a quest for a standard representation of inorganic layered structure types, as well as by González *et al.* (2011) in their study of pseudo-uniform orderings in two dimensions.

While recognizing the importance of the underlying principle for the systematic description of crystal structures, Iida (1957) restricted himself, rather unnecessarily, to hexagonal similar sublattices of small indices $T = 3, 4$ and 7 . And while neither Figueiredo (1973) nor Lima-de-Faria (1983) explicitly mention congruence relations in their respective approaches, Lima-de-Faria (1978) stresses that, for layer structures, the problem is better described as $(2 + 1)$ rather than three dimensional. Apart from the stacking of layers, which may be regarded as a problem of its own, the constitution of the individual layers can be reduced to an entirely two-dimensional problem. Indeed, many crystal structures, especially among intermetallic phases, are built from alternating flat and puckered layers, with the puckering often negligible, in which case the multiplicative congruential method is applicable without restrictions. Finally, González *et al.* (2011) show how pseudo-uniform grid-like orderings of a minority component in compositionally flexible compounds are triggered by the mutual self-avoidance due to repulsive interactions. In particular, these orderings can be described as (in)commensurately modulated structures with composition-dependent wavevectors and step-like modulation functions for the site occupancy. Modulation functions, too, satisfy one of the aforementioned criteria for a structural descriptor, being a mathematical tool encoding structural information in a most concise manner.

2.4. A quest for candidate structures

A preliminary search for candidate structures was most successful yet for some kinds of layered structures, representing the $(2 + 1)$ -dimensional case.

Work employing Pearson's database (Villars & Cenzual, 2007) suggests the compounds $\text{Pt}_{12}\text{Si}_5$ (dimorphous: room temperature = *tI34*, high temperature = *tP68*) and $\text{Ce}_5\text{Mg}_{41}$ (*tI92*) as tetragonal examples and Pu_3Pd_4 (*hR42*), Pr_7O_{12} (*hR57*), PdAl (*hR78*), CuSe (*hP156*), $\text{Cu}_{12.7}\text{Cr}_{19}\text{Al}_{83.8}$ (*hP244*), $\text{Sc}_6\text{Zr}_{25}\text{O}_{59}$ (*hR540*) as hexagonal ones. The decision as to whether a structure could be counted as a candidate was based on a visual inspection of parallel projections of the crystal structures along the axial direction of their respective hexagonal or tetragonal unit cells. In most cases the grid-like nature of their sublattice structure dominates this projection, even if in general several layers with slightly different atom distributions are stacked on top of each other perpendicular to the projection axis, thus blurring the impression. A greater number of representatives may be retrieved from the vast

amount of crystal structure data by – yet to be devised – refined search procedures.

Previously, another three hexagonal examples falling into this category were described, represented by the structures of $\text{Co}_2\text{Zn}_{15}$, IrZn_3 and Au_7In_3 , which crystallize in three structure types of their own, although sharing the same Pearson symbol $hP60$ (Hornfeck & Harbrecht, 2009; Hornfeck, 2010). Yet another hexagonal example, and the most complex found up to now, as indicated by its Pearson symbol $hP567$, is given by the amalgam $\text{Na}_{11}\text{Hg}_{52}$ [$P\bar{6}$ (No. 174), $a = 3970.3$ (2), $c = 968.10$ (5) pm, $Z = 9$], whose complex superstructure was recently elucidated by means of single-crystal X-ray diffraction (Hoch, 2010).

Finally, a comment should be made about the frequency of candidate structures constituted by layers of hexagonal and square symmetry. From a first glimpse it seems that hexagonal structures prevail, although the set of as yet identified candidate structures is still small. Nevertheless, a justification may be given based on the fact that the closest packing of equal spheres in two dimensions is the hexagonal one. For this reason one should expect to find a bias in favour of hexagonal structures.

3. Applications

Fundamentally, any MCG describes a mapping between a pair of coordinates (x, y) . Hence, MCGs are essentially two-dimensional in nature and best suited for the description of a flat (or, as is often the case, negligibly puckered) layer of atoms. However, generalizations to *three* dimensions are possible, where one may discern two cases:

(i) The $(2 + 1)$ -dimensional case. A suitable combination of *two* MCGs may be used to encode three-dimensional structures, according to the formula for a general coordinate triple:

$$\left[\underbrace{\frac{Z_i}{M}, \frac{mZ_i \pmod{M}}{M}}_{\text{rotational}}, \underbrace{\frac{nZ_i \pmod{N}}{N}}_{\text{translational}} \right] \equiv N_n^- \equiv N_{N-n}^+ \quad (8)$$

In fact, although at first composed of mere translations, this notation represents the rotational and translational part of the crystallographic N -fold screw axes ($N = 2, 3, 4, 6$). The crystallographic restriction has to be applied, since MCGs are defined on lattices. Note that the coordinates only depend on a single integer variable Z_i .

The geometrical interpretation is that of a combined coordinate shift defined on the unit cell of a three-dimensional lattice (*cf.* Fig. 1). Any point set (or, by analogy, atomic structure) whose elements can be reached successively *via* a constant shift vector with three, non-vanishing spatial components may be described by such a combination of two MCGs. Such an approach is nearly always possible, since most three-dimensional crystal structures may be formally dissected into an array of two-dimensional atomic layers.

(ii) The genuine three-dimensional case. The sublattice structure of an MCG is essentially a feature present in arbitrary dimensions. Thus, a three-dimensional coordinate vector

is simply given by merging three successive iterations of an MCG's output into the 3-tuple

$$(Z_n, Z_{n+1}, Z_{n+2}) \equiv (Z_n, mZ_n, m^2Z_n) \pmod{M} \quad (9)$$

In this way a single MCG, as a special case of a combination of two distinct MCGs (see above, employing the substitutions $N \rightarrow M$ and $n \rightarrow m^2$, where m^2 stands for the multiplier modulo M after the second iteration step), creates a lattice structure in three dimensions.

Both methods effectively give rise to a linearization of the three-dimensional structure under consideration (*cf.* §§3.2.1 and 3.3).

When it comes to the utilization of MCGs in relation to actual crystal structures, two approaches are discernible, depending on the objective in mind. Either

(i) to *idealize* the crystal structure to such an extent that it becomes possible to use an MCG with the smallest suitable modulus for its description, or

(ii) to make use of MCGs with ever-increasing moduli until a *rational approximation* of the real crystal structure to a desired precision is eventually reached.

Some cautionary notes shall be given regarding the usage of the terms *ideal* and *real*. Both refer to abstract structural models and their coordinate description in the first place, but make a distinction about their origin. Whenever we refer to structural models of actual crystal structures with a set of atomic coordinates originating from some structural refinement we will speak of *real* coordinates. As such they may be approximated to arbitrary precision by *ideal* coordinates generated by the action of an MCG. Thus, *ideal* does not refer to a perfect, infinitely extending ideal crystal, and *real* does not connote the real structure of a crystal, as may be visualized *e.g.* by electron microscopy.

Colloquially speaking, one either adjusts the structure description to the actual crystal structure [rational approximation; case (ii)] or proceeds the other way round [idealization; case (i)].

Both approaches are useful in their own way: the idealization of the crystal structure allows for the revelation of otherwise hidden structural relationships to more fundamental structures, whereas the rational approximation to a precision matching the experimental error margins makes it possible to store the numerical information given by the fractional atomic coordinates as determined in a diffraction experiment in a concise way.

It is important to note that the algorithmic complexity of the structural description by means of MCGs, *i.e.* the shortest way of encoding, is independent of either approach, since the number of crystallographic orbits to encode remains constant irrespective of the size of the chosen modulus.

3.1. Rational approximation of a layer structure

Because of a theorem of Dirichlet (Hardy & Wright, 2008; theorem 201, p. 218) it is always possible to simultaneously approximate a given set of real numbers to arbitrary precision by rationals sharing a *common denominator*. In our approach

the real numbers represent the actual atomic coordinates and the common denominator corresponds to the sublattice index (modulus) for the best-approximating sublattice (MCG). Fig. 2 depicts how selected crystallographic orbits of higher-index sublattices may be used to encode the deviations from the

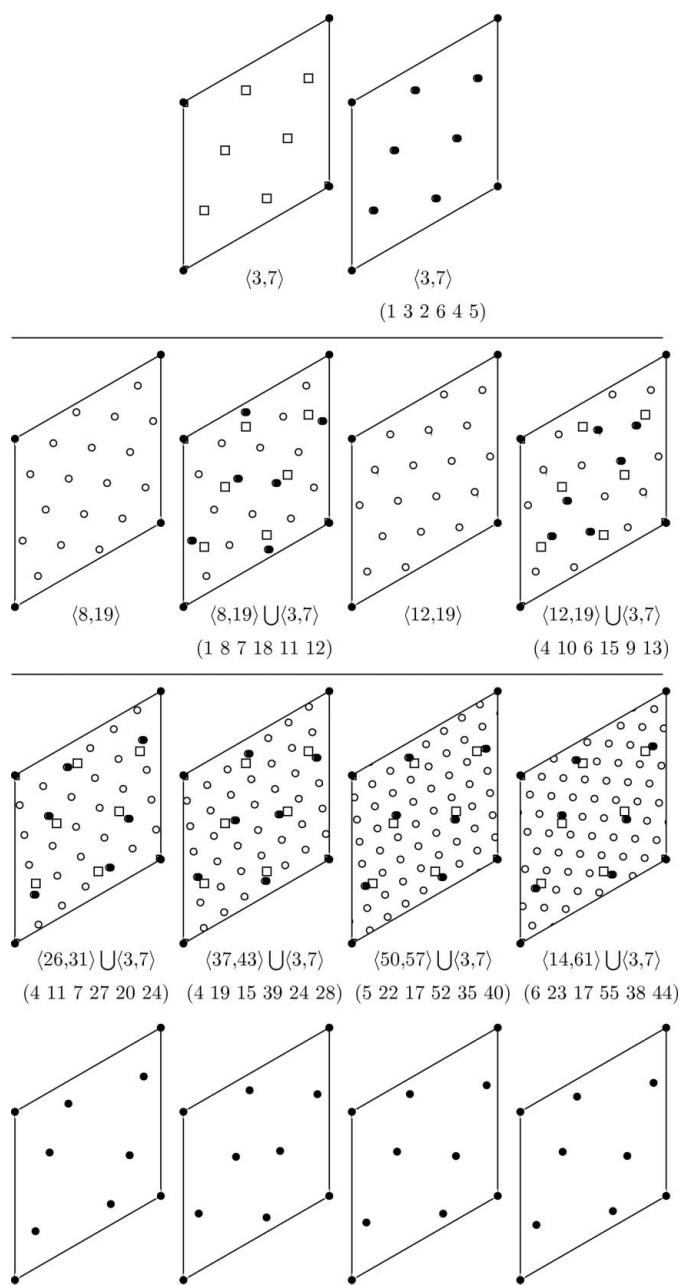


Figure 2
 First row: pair of hexagonal sublattices of index 7 with their single, ideal orbit highlighted. Second row: pair of enantiomorphous hexagonal sublattices of index 19 and their orbits that account for distinct deviations from the ideal orbit of the index-7 sublattice. Third row: single orbits of higher-index sublattices (higher-moduli MCGs) with $M = 31, 43$ and 57 that could be used to represent a spatially distorted ideal orbit of a hexagonal sublattice of index 7, associated with the MCG with $\langle m, M \rangle = \langle 3, 7 \rangle$. The symbol \cup denotes the union of two MCGs with respect to a common reference frame (here hexagonal unit cell).

ideal sites of a lower-index sublattice. The method will work as long as the actual crystal structure to be approximated can be conceived to be a superstructure of some basic structure, thereby establishing the necessary lattice–sublattice relationship.

A recourse to the properties of iterative maps (§A4) seems instructive too. For iterative maps an abounding number of rational starting values exist which result in periodic orbits (possibly of long period) having the same cycle length ℓ as for an MCG with integer-valued seed. These orbits may then be used for a description which diminishes the deviations up to a specified precision.

It is possible to optimize each crystallographic orbit separately, employing a number of distinct MCGs each with minimal modulus. Although such an optimization procedure possibly lengthens the description, in terms of the least necessary number of structural parameters, it eventually accounts for all deviations to an ideal superstructure.

The precision of a rational approximation may be calculated via a least-squares method applied to the distances between the approximate and actual atomic positions of the structure. For an MCG of given modulus and thus a sublattice of given index the maximal error corresponds to an atom lying at the barycentre of a fundamental mesh. Enlarging the modulus will minimize the deviations until eventually a perfect coincidence is reached for a given precision.

Experience shows that the atoms of actual crystal structures are usually located at sites nearby the nodes of the basic lattice, which represent the ideal coordinates of the superstructure, and that the observed deviations are therefore much smaller than the upper bound for the error might suggest.

3.2. Ideal representation of a three-dimensional structure

As was sketched before, it is, in principle, simple to generalize the concept of an MCG to more than two spatial dimensions. However, it is far from trivial to identify actual crystal structures, exemplifying the genuine three-dimensional rather than the $(2 + 1)$ -dimensional case. In contrast, it is simple to construct some artificial structure satisfying the constraints of the genuine three-dimensional case.

3.2.1. Construction of an artificial permutation structure.
 A simple example of an artificial structure may be obtained by the combination of two MCGs. For reasons of simplicity and without loss of generality we make the additional restrictions of having the two MCGs share the same modulus and cycle-length sequence. Thus, we choose the set

$$X \equiv X, Y \equiv 3X, Z \equiv 5X \pmod{7} \quad (10)$$

of congruence relations. Dividing these sets of integral coordinates by their common modulus yields the fractional coordinates $(x, y, z) = (X, Y, Z)/7$.

For the special case under consideration the two single MCGs describe a pair of enantiomorphous sublattices of index 7, similar sublattices, in fact, if embedded in a hexagonal reference frame (*cf.* Fig. 1). Except for the first, generating element of a cycle, only the positions of the other elements

within a cycle are reversed. Thus, one MCG defines the inverse permutation of the other, with the length of all cycles remaining unaffected.

The structure thus obtained is depicted at the top of Fig. 3, both as an abstract projection scheme, with the (x, y) coordinates and the heights in the upwardly oriented z direction given as integers, and as a tilted view of a three-dimensional bar plot, with shaded cubes representing the atomic sites. This

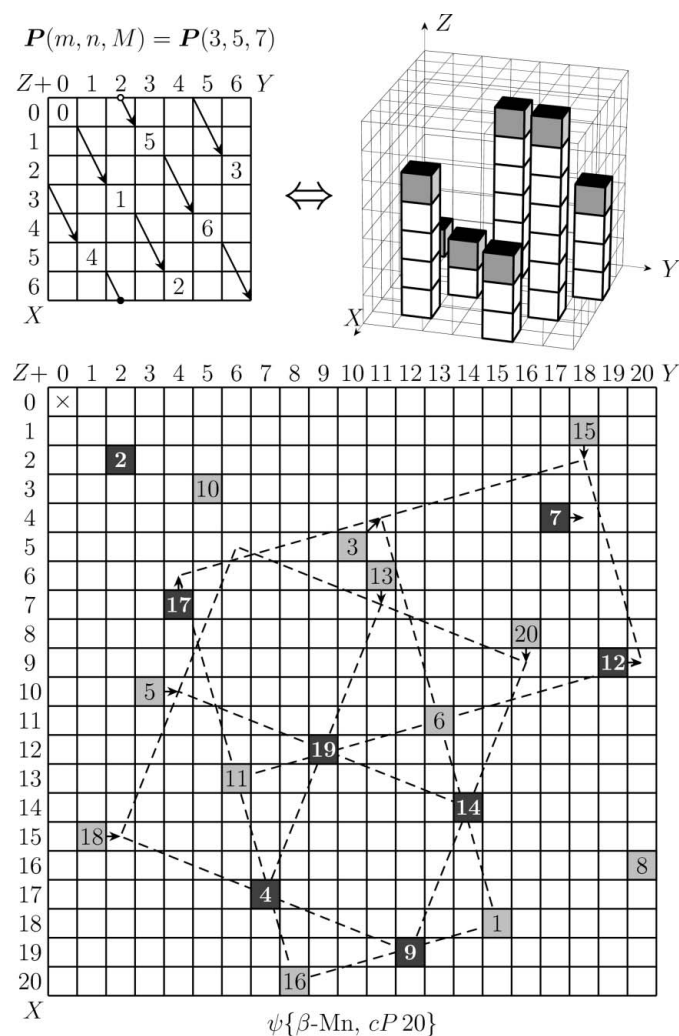


Figure 3

Top: abstract point structure generated by the combined action of two MCGs, $Y \equiv 3X \pmod{7}$ and $Z \equiv 5X \pmod{7}$, i.e. with the distinct multipliers $m = 3$ and $n = 5$ and a common modulus $M = 7$. The structure is shown once in projection (left side) with the heights in the z direction given by the numerator of the rational coordinate values (with a common denominator of 7) and another time as a three-dimensional bar plot, with shaded cubes representing the points (right side). Note that the cubes are distributed in such a way that the structure may be regarded as a generalization of a permutation matrix to three dimensions. Bottom: idealization of the β -Mn-type structure choosing a similar two-dimensional representation as before (Wyckoff sites 8c and 12d shaded dark and light grey, respectively), disregarding the proper symmetry relations between equivalent sites while emphasizing its near-miss character as a three-dimensional permutation structure. Note also the near-miss character regarding the distribution of sites (in projection) relative to the sketched sublattice meshes (dashed lines), whose edge lengths are nearly incommensurate by a factor of $2^{1/2}$.

construction, in its most isotropic metrical embedding, yields a cubic unit cell which has similar projections along all of its principal axes. An analysis of mutual coordination shows that atoms in such a structure would be distributed quite uniformly. Because of its spatial homogeneity, one is tempted to speculate if such a structure could be realized. A search for symmetry employing the *ADDSYM* subroutine of the *PLATON* suite (Spek, 2009) shows the presence of a threefold inversion axis, with the cubic unit cell in fact representing the primitive unit cell for a trigonal, R -centred structure better described with hexagonal axes in space group $R\bar{3}$ (No. 148). Corresponding to the number of cycles in the MCG's cycle representation two distinct sites are occupied, i.e. $3a(0, 0, 0)$ and $18f(x, y, z) = (1/7, 3/7, 0)$, with a total of $3 \times 7 = 21$ atoms within the R cell.

This artificial structure is remarkable for another two features:

(i) As a consequence of its construction the structure can be regarded as a three-dimensional generalization of a two-dimensional permutation matrix, since all possible sites are vacant, except for a single occupied site in every row $[u, 0, 0]$, column $[0, v, 0]$ and rod $[0, 0, w]$. Accordingly, we propose to name such crystal structures *permutation structures*.

(ii) In addition, the structure exemplifies a *linearization procedure*, in that all atoms are passed along a linear path, e.g. along the cubic $[3, 2, 1]$ direction, as indicated by arrows in the top left scheme of Fig. 3.

The latter feature will be discussed in detail in §3.3.

3.2.2. Near-miss permutation structure of β -Mn. Following the aforementioned rationale the question arises of whether permutation structures exist among the actual known crystal structures.

Although no perfect match has been found until now, and it is not yet even clear how to effectively search for it, a near-miss candidate does exist: namely, the peculiar structure of β -Mn. This allotrope of Mn crystallizes in one of the *chiral* cubic space-group types $P4_132$ (No. 213) and $P4_332$ (No. 212) with the primitive unit cell comprising 20 atoms (Pearson symbol $cP20$), two of which form an asymmetric unit (Wyckoff positions Mn1: $8c; x, x, x$ and Mn2: $12d; 1/8, y, y + 1/4$). The structure was previously described as a body-centred cubic, garnet-type rod packing of chains of Mn_1Mn_2_3 tetrahedra combined with Mn_2_6 triangular metaprisms (the shape of a metaprism is in between that of a triangular prism and antiprism, with an intermediate angular offset regarding the opposite basal planes). Under the assumption of a most uniform distribution of interatomic distances ideal parameters were derived to: $x = 1/(9 + 33^{1/2}) \simeq 0.0678$ and $y = (9 - 33^{1/2})/16 \simeq 0.2035$ (O'Keeffe & Andersson, 1977). An alternative description from Nyman *et al.* (1991) describes the β -Mn structure as a primitive rectilinear rod packing of a polyhedral helix solely composed of nearly regular, face-sharing tetrahedra. Both rod packings differ in the crystallographic directions to which the rods are aligned (O'Keeffe, 1992).

Within our approach an idealized structure of β -Mn is depicted as a permutation structure, in a similar fashion as

already shown in Fig. 3, *i.e.* as a bar plot encoded in an abstract two-dimensional projection scheme. Atoms corresponding to the Wyckoff sites $8c$ and $12d$ are shaded dark and light grey, respectively. However, the proper cubic symmetry relations have to be discarded completely, such that all sites in fact represent the general position of space group $P1$ (No. 1).

The ideal permutation structure of a near-miss β -Mn-type structure is given by the cycle representation

$$\begin{aligned} &(0)(1\ 18\ 15)(2)(3\ 5\ 10)(4\ 17\ 7) \\ &(6\ 11\ 13)(8\ 16\ 20)(9\ 19\ 12)(14) \end{aligned} \quad (11)$$

Since, apart from fixpoints located at (x, x, x) , only cycles of length three occur, the cycle representation seems to be related to a threefold rotation perpendicular to a cubic body diagonal. However, no obvious construction by means of two MCGs, as exemplified for the artificial model of §3.2.1, has been figured out yet. Accordingly, the existence of a linearization procedure is uncertain, though still a matter of assumption.

The ideal positions of the permutation structure deviate to a variable extent from the refined ones for the actual crystal structure of β -Mn. The permutation structure can be seen as an equi-distributed, ‘average’ structure.

The near-miss character is evident in diverse details of the projected structure, *e.g.* regarding the distribution of atoms to two independent square sublattices, sketched by dashed lines in Fig. 3. Both sublattices almost relate to each other by the classical construction of nested squares, where a smaller square is inscribed into a larger one such that their respective edge lengths scale in the ideal, incommensurate ratio of $1:2^{1/2}$ (the ratio 8:12 of the site multiplicities may be seen as an approximation of this irrational ratio). Denoted by their heights the smaller square is composed of the points at $z = 4, 9, 14, 19$, with the larger one at $z = 1, 6, 11, 16$. The distance in z corresponds approximately to the translational part of a 4_1 screw axis. However, there is a mismatch concerning the orientation of adjacent nested squares, which are related by symmetry in the actual structure of β -Mn. For instance, the atom at $z = 20$ could be either part of a sublattice of small squares defined by the atoms at $z = 9$ and $z = 14$ or equally well part of a sublattice of large squares defined by itself and the atom at $z = 15$.

Incommensurate length scales are a characteristic phenomenon exhibited by quasicrystals and quasicrystal approximants. Indeed, β -Mn is the approximant structure of an octagonal quasicrystal with two-dimensional quasi-periodicity and a structure corresponding to an Ammann–Beenker-type tessellation (Elenius *et al.*, 2009).

The major discrepancy of the model lies in the fact that the Wyckoff position $12d$ is a special position with a restraint in one coordinate value to multiples of $1/8$, which are symmetry-wise inconsistent with multiples of $1/21$, except for a structure grossly reduced in symmetry (*i.e.* $P1$). A possible remedy would be to use sublattices of much higher index instead, *e.g.* by means of employing common multiples of the Wyckoff multiplicities. However, under these circumstances a com-

paratively large amount of vacancies has to be introduced, yielding a diluted or sparse permutation structure.

Finally, it has not escaped our notice that a ‘bar plot’-type model of the β -Mn structure had been devised by Chapman as early as about 1952 at the Crystallography Department of the Cavendish Laboratory at the University of Cambridge (see Hyslop, 2008 for a picture), albeit without giving an explicit reference to the structure’s permutation-like character.

3.3. Algorithmic generation of crystal structures

Besides their possible application for the concise and size-independent numerical encoding of crystal structure information, MCGs may also be used for a systematic, *i.e.* an algorithmic, generation of crystal structures. The idea behind this may be sketched as follows.

Given a fixed modulus M any multiplier $m \in \mathbb{Z}/M\mathbb{Z}$ imposes a corresponding cycle representation. A single cycle, closed under subsequent transformations of the MCG, represents a single crystallographic site, closed under a certain symmetry. A site may be either occupied by some type of atom (\bullet) or empty, *i.e.* occupied by a formal vacancy (\circ). Once an MCG description is found for a certain crystal structure, employing two distinct multipliers (coordinate shifts) m and n and, possibly but not necessarily, two distinct moduli (sublattice periodicities) M and N for a three-dimensional structure, the structure may be *linearized* accordingly. Afterwards, the linear sequence of sites and its occupancy pattern (*e.g.* $\bullet \circ \bullet \bullet \bullet$) define a binary string (or ternary *etc.* depending on the number of atom types including vacancies), an occupancy sequence, such as $(10111)_2$, which may be further compactified by giving its decimal value $(23)_{10}$.

It should be noted that the structures thus obtained already share some characteristic of actual crystal structures, as a consequence of their construction from the sublattice structure of MCGs, in that the sites and hence the atoms are spatially distributed in a uniform manner. Therefore this approach of algorithmic structure generation differs from other ones that yield a more random distribution of atomic sites instead.

The two most notable aspects of this approach are as follows:

(i) Crystal structure linearization. At first glance a linearization of a three-dimensional crystal structure seems disadvantageous, since naturally most of the crystal chemical information concerning the exact nature of the spatial arrangement of atoms will get obscured, to say the least. However, within the framework of the multiplicative congruential method no information is really lost, since the construction is bijective. Thus, any three-dimensional information may be fully reconstructed at any time. On the contrary, a linearization procedure has some major advantages, especially in terms of electronic data storage, retrieval and evaluation. For this very reason several linearization procedures, such as Wiswesser line notation or SMILES have been invented for molecular compounds (Wiswesser, 1985; Weininger, 1988).

(ii) Combinatorial crystallography. The multiplicative congruential method not only offers a way for the generation of candidate structures for actual crystal structures, but also offers a *systematic* way of doing so, instead. For instance, regarding the generation of a series of crystal structures, the multiplier of an MCG may be varied systematically while its modulus remains fixed, whereas the additional variation of the modulus (sublattice index) imposes a natural hierarchy among the generated structures, analogous to the well known group–subgroup relationships between space-group types. A systematic generation of crystal structures thus, at the same time, gives an exhaustive enumeration of possible (super-)structures as well as a hierarchical classification scheme for them. Again, similar approaches are well established in molecular chemistry, starting from Cayley’s pioneering work on the enumeration of the constitutional isomers of the alkanes to modern computational approaches like the *MOLGEN* project (Kerber *et al.*, 2004; Gugisch *et al.*, 2007).

In such a way MCGs, together with a combinatorial array of occupancy sequences, may be used in the field of chemical crystallography to specify the spatial arrangement of atoms in arbitrary three-dimensional structures.

4. Outlook

4.1. Back and forth to number theory and crystallography

Permutations of the type $Z_i \mapsto mZ_i \pmod{M}$ with $Z_i \in \mathbb{Z}/M\mathbb{Z}$ and $\gcd(m, M) = 1$ play a significant role in number theory, *e.g.* as a relevant part in an elementary proof of the Fermat–Euler theorem (Hardy & Wright, 2008, p. 78). The corresponding permutation matrices $\mathbf{P}(m, M)$, of which equation (5) gives an example, are generalizations of *circulant matrices*. An m circulant is an $M \times M$ matrix such that each row (except the first) is obtained from the preceding by shifting each element m positions to the right (Brenner, 1973).

In yet another manner an MCG may impart a relation between certain sets of integers, termed *Singer difference sets*, which are n -element subsets of $\mathbb{Z}/M\mathbb{Z}$, where the modulus is

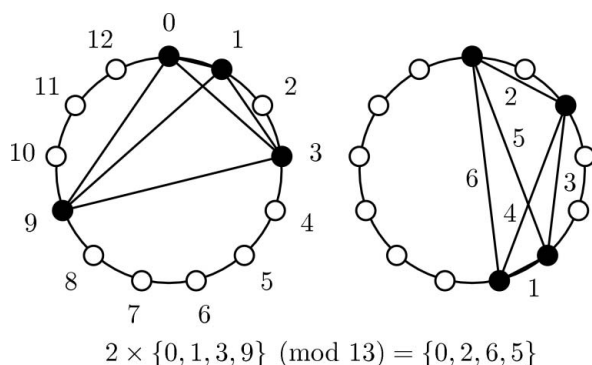


Figure 4

Homometric cyclotomic sets related by the action of an MCG. Shown in the left diagram is the clockwise ascending enumeration and labelling of the line lattice nodes, to which the notation of the difference sets refers, whereas on the right diagram the set of interpoint distances, given as multiples of a unit chord length, is emphasized.

given as $M = (q^3 - 1)/(q - 1)$, $q = n - 1$ is a prime power and each set’s distance set is composed of the $M - 1 = n(n - 1)$ non-zero elements of $\mathbb{Z}/M\mathbb{Z}$ appearing exactly once (Lemke *et al.*, 2002). Sharing the same distance set is a necessary but not sufficient condition for two or more point sets to be *homometric*, since two or more of such point sets may alternatively either be congruent or enantiomorphic to one another. A special class of homometric sets in one spatial dimension was intensively studied by Patterson (1944), for which he coined the name *cyclotomic sets* in regard to the solutions of the cyclotomic equation $z^n = 1$ ($z \in \mathbb{C}$).

An example of such a relation is given by the MCG

$$Z_{n+1} \equiv 2Z_n \pmod{13}, \quad (12)$$

with

$$(0)(1\ 2\ 4\ 8\ 3\ 6\ 12\ 11\ 9\ 5\ 10\ 7) \quad (13)$$

as its associated cycle representation, iteratively applied to the set $\{0, 1, 3, 9\}$. One can easily assure oneself, using the graphical method depicted in Fig. 4, that two out of four distinguishable sets are distinct entities representing the same distance set and thus are homometric to each other, while the other two sets are mere reflections of the former. The cyclotomic point sets devised by Patterson highlighted the complementary nature of a certain class of homometric structures. A construction due to Zobetz (1993) generalized this to two dimensions, founded on what he called *kommensurable Mehrfachgitter* (commensurate multilattices), and what in fact are general sublattices with an even number of basic lattice nodes confined within a sublattice unit mesh (and thus an odd sublattice index), such that an equipartition into two complementary point sets is possible, which may then form a homometric pair.

4.2. MCGs in dual space

Any lattice–sublattice relationship in direct (real) space corresponds to a lattice–superlattice relationship in dual (reciprocal) space. Accordingly, the Wyckoff positions of direct space have a counterpart in dual space, termed *Wintgen positions* (Wintgen, 1941). Thus, it seems possible, at first glance, to directly transfer all the aforementioned ideas regarding the use of MCGs in direct space to dual space. As an MCG in real space defines a mapping of a Wyckoff position’s coordinates onto another, one should expect a similar mapping in reciprocal space, namely for the \mathbf{k} -vector coefficients of a Wintgen position [*International Tables for Crystallography*, Vol. B (2nd ed.), ch. 1.5], with possible ramifications regarding the simplification of the phase-angle term in the complex expression of the structure-factor equation.

5. Conclusion

MCGs were previously introduced for the coordinate description of ideal, two-dimensional superstructures, for which the atomic sites had to be in exact registry with the underlying basic lattice nodes.

A twofold extension was developed within this paper in order to treat the more realistic cases of non-ideal, three-dimensional superstructures, thereby facilitating the use of MCGs as quantitative crystal structure descriptors. In particular, two strategies were introduced of either adjusting an actual crystal structure or its description by a structural model to one another until their relative mismatch is minimized with respect to a given precision. Furthermore, a method was sketched for the algorithmic generation of crystal structures by means of MCGs employing an inherent linearization procedure for their combinatorial enumeration.

MCGs have their concomitant virtues, since matrix algebra does not have to be invoked in order to calculate sets of transformed coordinates resulting from a lattice–sublattice transformation, nor does their associated algorithmic complexity rise with its index. Instead, it merely takes a pair of integers, the multiplier and the modulus of an MCG, in order to encode all the necessary numerical information about an actual crystal structure’s coordinates. Moreover, it involves nothing more than applying subsequent multiplications alter-

nating with division with a remainder to generate all crystallographic orbits explicitly, preserving their point-group symmetry – algebra which can be done by pen and paper.

Thus, it is our conviction that MCGs offer a viable way of encoding the structural complexity of a given crystal structure into a single, yet quantitative, crystal structure descriptor.

APPENDIX A Generalizations and extensions

A1. Primitive sublattices of arbitrary symmetry

Although the first treatment of MCGs within the crystallographic realm was largely restricted to similar sublattices of hexagonal and square symmetry, the concept seems practical for any lattice–sublattice relation in general, independent of a given symmetry or spatial dimension, as long as the sublattice under consideration is a *primitive* – but not necessarily similar – one, including any of the non-centred, two-dimensional Bravais lattices (Fig. 5, top), as well as their higher-dimensional analogues.

The reason for this is given by the bijective character of the mapping, assigning each sublattice point its unique pair of integral coordinates. On the contrary, any non-primitive sublattice contains several lattice points that violate this condition, due to the existence of additional centring translations. This argument generalizes in a straightforward manner to non-primitive sublattices in any dimension.

It is therefore possible to cover a much greater parameter space (Fig. 5, bottom) than before. It seems especially interesting to study the restrictions imposed on an MCG’s parameter set by the symmetry of the basic lattice, as well as the invariance of the multiplier m , or an eventual breaking thereof, under affine transformations of the underlying lattice.

A2. Geometric algebra description of MCGs

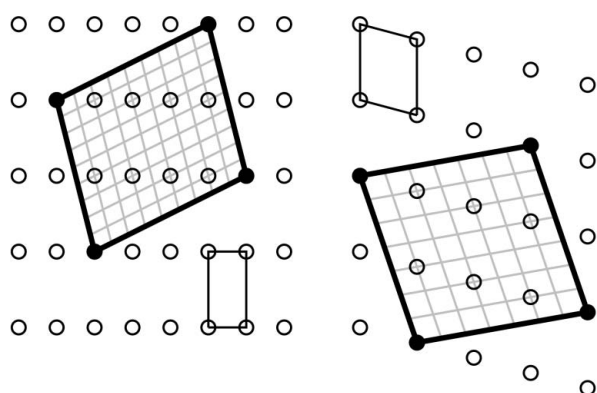
The transformation of the basic vectors of a given lattice Λ into the ones of its sublattice Λ' is described by means of matrix algebra as

$$(\mathbf{A}, \mathbf{B})_{\Lambda'} = (\mathbf{a}, \mathbf{b})_{\Lambda} \mathbf{M}, \quad \mathbf{M} = \begin{pmatrix} p & q \\ r & s \end{pmatrix}. \quad (14)$$

The integer modulus M of an associated MCG is directly determined as the index of the lattice–sublattice transformation, *i.e.* as the value of the determinant of the above transformation matrix, $M = \det \mathbf{M}$.

The integer multiplier m , however, is less directly obtainable, despite being restricted to the interval $[1, M - 1]$. It has to be determined from the unknown lattice vector $\sigma = (u, v)^t$ (with the superscript ‘t’ denoting a transposition), extending from the origin to the lattice point closest to the line segment defined by the transformed lattice vector \mathbf{B} , *via* the defining equations

$$u = (p + \mu q)M^{-1} \quad v = (r + \mu s)M^{-1} \quad (15)$$



$$Z_{n+1} \equiv 2 Z_n \pmod{9} \quad Z_{n+1} \equiv 3 Z_n \pmod{7}$$

$$(0)(1 \ 2 \ 4 \ 8 \ 7 \ 5)(3 \ 6) \quad (0)(1 \ 3 \ 2 \ 6 \ 4 \ 5)$$

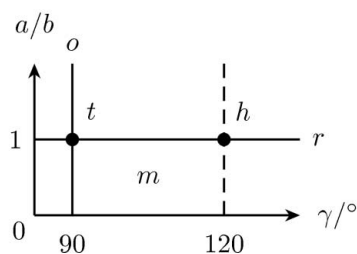


Figure 5

Top: dissimilar primitive sublattices of basic lattices with rectangular and oblique symmetry, respectively, shown together with their corresponding MCGs and cycle representations. Bottom: parameter space of two-dimensional lattices given by the axial ratio a/b and the angle γ . The parameter space of lattices with hexagonal (h) and square (t) symmetry is zero-dimensional (a point), the one of rectangular (o) and centred rectangular (r) lattices is one-dimensional (a line) and the one of oblique (m) lattices is two-dimensional (the plane). Any point of the parameter space may be reached by means of affine transformations of a given lattice.

[cf. equation (16) in Hornfeck & Harbrecht, 2009]. Now, one may solve for the multiplier μ by substituting one equation into the other, thereby eliminating the modulus M common to both:

$$\mu = \frac{pv - ru}{us - vq} = \frac{\det \begin{pmatrix} p & u \\ r & v \end{pmatrix}}{\det \begin{pmatrix} u & q \\ v & s \end{pmatrix}} \Leftrightarrow \frac{|\mathbf{A} \wedge \boldsymbol{\sigma}|}{|\boldsymbol{\sigma} \wedge \mathbf{B}|} = \frac{\mu}{1}. \quad (16)$$

At first sight there seems nothing new, since the variables u and v are still unknown.

However, one may identify both numerator and denominator with the determinant of a 2×2 matrix. Furthermore these matrices are each composed of a pair of vectors, namely one of the transformed basic vectors, \mathbf{A} or \mathbf{B} , of the sublattice Λ' together with the unknown vector $\boldsymbol{\sigma}$. Thus, both determinants represent the areas of the lattice meshes spanned by these vectors.

This insight may be represented within the language of *geometric algebra*. Being a generalization of matrix algebra the well known scalar product $\mathbf{x} \cdot \mathbf{y} = |\mathbf{x}||\mathbf{y}| \cos \gamma_{\mathbf{xy}}$, defined between two vectors \mathbf{x} and \mathbf{y} , is accompanied by a complementary wedge product $\mathbf{x} \wedge \mathbf{y} = |\mathbf{x}||\mathbf{y}| \sin \gamma_{\mathbf{xy}}$, yielding a *bivector*, i.e. a geometric object representing an *oriented area*, whose magnitude $|\mathbf{x} \wedge \mathbf{y}|$ is a scalar measure of its spatial extension (Dorst *et al.*, 2007).

Since the vector $\boldsymbol{\sigma}$ by definition represents the lattice point closest to the line segment given by the basic vector \mathbf{B} , the mesh spanned by both vectors describes a fundamental mesh of the lattice Λ , hence is of unit area, $|\boldsymbol{\sigma} \wedge \mathbf{B}| = 1$ (otherwise there would be at least another lattice point lying in this mesh, which would be closer to the aforementioned line segment,

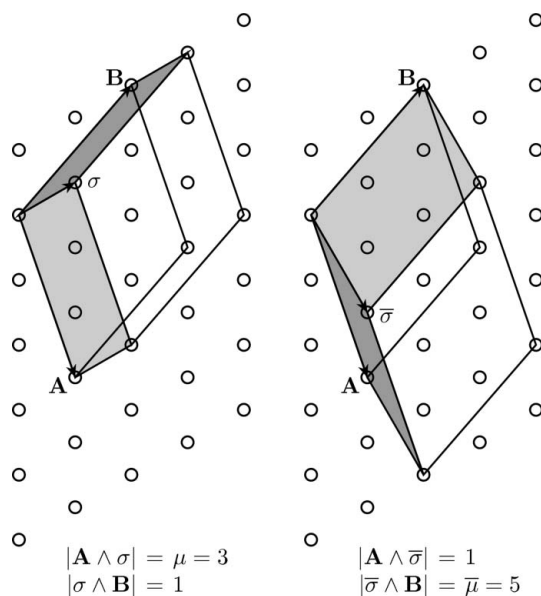


Figure 6
Wedge products of lattice vectors – shown for a hexagonal similar sublattice corresponding to the MCG with $m = 3$ and $M = 7$ – and their geometric interpretation as lattice meshes of defined area (shaded light and dark grey), thus yielding the special multipliers μ and $\bar{\mu}$ as results.

which is a contradiction to the definition of $\boldsymbol{\sigma}$). As a logical consequence, the expression $|\mathbf{A} \wedge \boldsymbol{\sigma}|$ describes a lattice mesh of area μ , giving the multiplier a similar geometric meaning as the modulus (Fig. 6), for which $|\mathbf{A} \wedge \mathbf{B}| = M$. In this way the linear nature of the length ratio m/M , originating from the definition given in equation (2) and representing two distinct translations, transcends into two dimensions and a ratio m/M of areas. Since geometrical algebra easily generalizes to spaces of any dimension similar results are expected for three-dimensional space. For example, the concatenation of the wedge product, $|\mathbf{A} \wedge \mathbf{B} \wedge \mathbf{C}|$, with $\mathbf{A}, \mathbf{B}, \mathbf{C}$ some basic vectors of a three-dimensional sublattice, allows the simple calculation of its index.

A3. General cycle representation of MCGs

The MCG-induced cycle structure preserves the rotation symmetry of the underlying two-dimensional lattice, regarding any combination of the multiplier m for a fixed modulus M (Hornfeck & Harbrecht, 2009; the special multipliers μ and $\bar{\mu}$, however, correspond to the rotational symmetry operations of highest order and thus the cycles of maximal length). The rotation can then be expressed in matrix form as

$$\begin{pmatrix} Z_{n+1} \\ Z_{n+2} \end{pmatrix} = \mathbf{R} \begin{pmatrix} Z_n \\ Z_{n+1} \end{pmatrix} \quad (17)$$

with \mathbf{R} a 2×2 rotation matrix. For an N -fold rotation the general formula

$$\begin{pmatrix} Z_{n+m} \\ Z_{n+m+1} \end{pmatrix} = \mathbf{R}^m \begin{pmatrix} Z_n \\ Z_{n+1} \end{pmatrix} \quad (18)$$

holds true, with $\mathbf{R}^N = \mathbf{I}$, where \mathbf{I} is the identity matrix. At this point it seems useful to remember that successive elements of a cycle are regarded as a coordinate pair, e.g. $(X, Y) = (Z_n, Z_{n+1})$. Thus, the matrix multiplication with \mathbf{R} acts in an equivalent way as the MCG. From this it is possible to calculate all elements of a cycle from the knowledge of the special multiplier μ alone.

For a similar sublattice with hexagonal or square symmetry the rotation matrix for a clockwise, i.e. negative sense, rotation is given by

$$\mathbf{R}(6^-) = \begin{pmatrix} 0 & 1 \\ -1 & 1 \end{pmatrix} \quad \text{or} \quad \mathbf{R}(4^-) = \begin{pmatrix} 0 & 1 \\ -1 & 0 \end{pmatrix}, \quad (19)$$

respectively. Applying the matrices in the aforementioned manner gives (for the hexagonal case)

$$\begin{pmatrix} Z_{n+1} \\ Z_{n+2} \end{pmatrix} = \begin{pmatrix} 0 & 1 \\ -1 & 1 \end{pmatrix} \begin{pmatrix} Z_n \\ Z_{n+1} \end{pmatrix}. \quad (20)$$

Writing out the second line yields the *difference equation*

$$Z_{n+2} = -Z_n + Z_{n+1} \quad (21)$$

where an integer value is given by the sum of the two preceding values in the sequence (or, equivalently, by the first two values of the sequence, if higher matrix powers are considered). Regarding recurrence relations, a difference equation is the discrete analogue to a differential equation in

the context of functions. Using the definition of equation (2) (for a special multiplier $m = \mu$) one gets

$$Z_{n+2} = -Z_n + \mu Z_n = (\mu - 1)Z_n \pmod{T}. \quad (22)$$

From the recursion follows

$$Z_{n+2} \equiv \mu Z_{n+1} \equiv \mu(\mu Z_n) \equiv \mu^2 Z_n \pmod{T} \quad (23)$$

and thus, by comparison of factors, $\mu^2 = \mu - 1 \pmod{T}$ (corresponding relations can be deduced for other powers of μ in a similar fashion). In a general notation, the cycle with seed value $Z_1 = 1$ is given by $(1 \mu \mu^2 \mu^3 \mu^4 \mu^5) \pmod{T}$ with $\mu^6 \equiv 1 \pmod{T}$. Exploring all difference equations resulting from equations with distinct $N = 0, 1, \dots, 5$ yields

$$[1 \mu (\mu - 1)(-1)(-\mu)(-\mu + 1)] \pmod{T} \quad (24)$$

with the elements of the cycle as the results of the closed-form solution to the general recurrence formula [equation (21) together with $Z_1 = 1, Z_2 = \mu$] for hexagonal MCGs:

$$Z_n(\mu)_{\text{hex}} = (1 - \mu) \cos\left(\frac{n\pi}{3}\right) + \frac{1}{3^{1/2}}(1 + \mu) \sin\left(\frac{n\pi}{3}\right). \quad (25)$$

The calculation in the square case is analogous, resulting in

$$(\mu^0 \mu^1 \mu^2 \mu^3) \equiv [1 \mu (-1)(-\mu)] \pmod{Q}, \quad (26)$$

with $\mu^4 \equiv 1 \pmod{Q}$, and the solution formula for square MCGs:

$$Z_n(\mu)_{\text{squ}} = -\mu \cos\left(\frac{n\pi}{2}\right) + \sin\left(\frac{n\pi}{2}\right). \quad (27)$$

These results allow for simple proofs of the conjectures regarding the relation between $\mu, \bar{\mu}$ and their respective sublattice indices T or Q as stated in Hornfeck & Harbrecht, 2009 (§9): from $\bar{\mu} \equiv \mu^{\ell-1} \equiv -\mu + 1 \pmod{T}$ and $-\mu \equiv T - \mu \pmod{T}$ follows $\mu + \bar{\mu} = T + 1 \pmod{T}$ for the hexagonal case, and similarly $\mu + \bar{\mu} = Q \pmod{Q}$ for the square one.

A4. MCGs as iterative maps

The action of any given MCG may be presented and evaluated graphically employing a Cartesian coordinate system. Within this reference frame an MCG defined by the congruence $y \equiv mx \pmod{M}$ is conceived as a piecewise linear function of the variable x , *i.e.* a line intersecting the origin, with a slope given by the multiplier m , which is chopped and down-projected in steps of the modulus M . For values of x exceeding the value of the modulus M there is a periodic repetition, such that it suffices to look at the interval $[0, M)$ in both axis directions x and y . In order to establish the recursive behaviour of the mapping and to study its dynamical behaviour another linear function is needed, namely $y = x$ with unit slope. The resulting diagram, where any point on the abscissa is alternately mapped to a point on the line $y = mx \pmod{M}$ (*i.e.* $x \mapsto y$) and afterwards to the line $y = x$ (*i.e.* $y \mapsto x'$), is known as a *cobweb* plot.

Cobweb plots are widely used to study and depict the behaviour of iterative functions and their discrete dynamics in

a graphical, semi-quantitative way (Alligood *et al.*, 1996). One of the most studied examples is the *logistic map* (May, 1976)

$$x_{n+1} = rx_n(1 - x_n) \quad (28)$$

where $0 < r \leq 4$, and another well known example is the *Bernoulli map*, also known under a plethora of other names, *e.g.* as a bit shift map (because that is what effectively happens if the iterations are written in their binary expansion) or dyadic transformation

$$z_{n+1} \equiv Dz_n \pmod{1}, \quad (D = 2), \quad (29)$$

which is topologically conjugate, *via* the coordinate transformation $x_n = \sin^2(2\pi z_n)$, to the $r = 4$ case of the logistic map, where chaos prevails. Both maps are exactly solvable, with

$$z_{n+1} = \frac{1}{\pi} \cot^{-1} \left[\cot(2^{n+1} \pi z_0) \right] \quad (30)$$

the analytical expression for the solutions of the Bernoulli map (Katsura & Fukuda, 1985). The Bernoulli map and its generalizations with $D > 2$ are well known for their chaotic behaviour and it is easy to recognize and establish their relation to MCGs (Herring & Palmore, 1989; Palmore & Herring, 1990; Konno & Kondo, 1997).

A simple graphical corollary from this plot is that the intersection of both functions directly yields the fixpoints of the mapping whereas any periodic orbit is represented by a closed trajectory (Fig. 7).

The orbits for integer starting values (seeds) are always periodic (fixpoints are period-one orbits). For nearby located seeds a quite distinct behaviour is observed, using the same MCG as before. Then, one immediately recognizes that the dynamic behaviour exhibits a sensitive dependence on the initial conditions (*i.e.* the chosen seed) which is one of the telling signs on the way into chaos (Fig. 7). If the seed is rational the corresponding orbit of the MCG-related iterative map is eventually periodic (probably with a large period), whereas an irrational seed yields a chaotic orbit (since the map in the case of an MCG is piecewise linear the chaotic movement is always ergodic; Konno & Kondo, 1997). This is of some importance for the approximation of real-structure coordinates by means of MCGs. The sensitive dependence on the initial conditions is some characteristic feature of iterative maps and is discussed in detail and in the more general context of cellular automata for the case of the bit shift map $z_{n+1} \equiv 2z_n \pmod{1}$ by Wolfram (2002, pp. 149–155). A large body of observations suggests that an arbitrary cellular automaton (including iterative maps) falls into one out of only four distinct complexity classes regarding its behaviour when started from random initial conditions, where class 4 comprises the most complex cases (pp. 231–245). MCGs fit into this empirical classification scheme as ‘Systems of Limited Size and Class 2 Behavior’, where class-2 systems are chiefly characterized by their lack of long-range communication and their eventually repetitive behaviour (pp. 255–260). Complexity in these systems arises more by the complexity (or randomness) of their input, rather than from their inherent properties (transformation rules of the mapping).

A5. MCGs and codimension-one quasicrystal approximants

The basic idea behind modular arithmetics is to introduce a congruence relation defined on the integers $Z' \equiv Z \pmod{M}$, with Z and Z' sharing the same remainder after division by the modulus, *i.e.* their difference being an integer multiple of M . In a slightly different view, commonly adopted in computer science, the congruence relation is interpreted as a *functional*

relationship, *i.e.* a modulo operation $y = x \pmod{M}$. Depicted on the number line this may be viewed either as translational equivalence of integer coordinates with a translation period M (thinking of a congruence relation), or as a back-projection of integers into a unit interval, the size of which is defined by the modulus M (thinking of a modulo operation). In both cases the modulus M acts as a one-dimensional translation operation.

The simplest quasicrystals imaginable, the ones exhibiting one-dimensional quasiperiodicity, may also be depicted on a number line. In many cases these are derived from the Fibonacci sequence of integers. For such one-dimensional quasicrystals explicit coordinates may be given as a closed-form analytical expression, which establishes a one-to-one correspondence between a set of site coordinates and a set of indices enumerating the sites according to some ordering scheme. The same is true for one-dimensional codimension-one *quasicrystal approximants* (Mosseri, 1988; Duneau *et al.*, 1989; Sadoc & Mosseri, 1999; Vidal & Mosseri, 2000). In these cases, seemingly not noticed before, the expression takes the appearance of an MCG. This has a subtle advantage, which is valid for all codimension-one quasicrystals and can be extended to higher codimensions, in that the MCG's action defines a natural ordering scheme for the sites, dubbed as conumbering before, due to the fact that the site indices represent distances in the perpendicular space, *i.e.* distances to the sublattice nodes, as illustrated in Fig. 8.

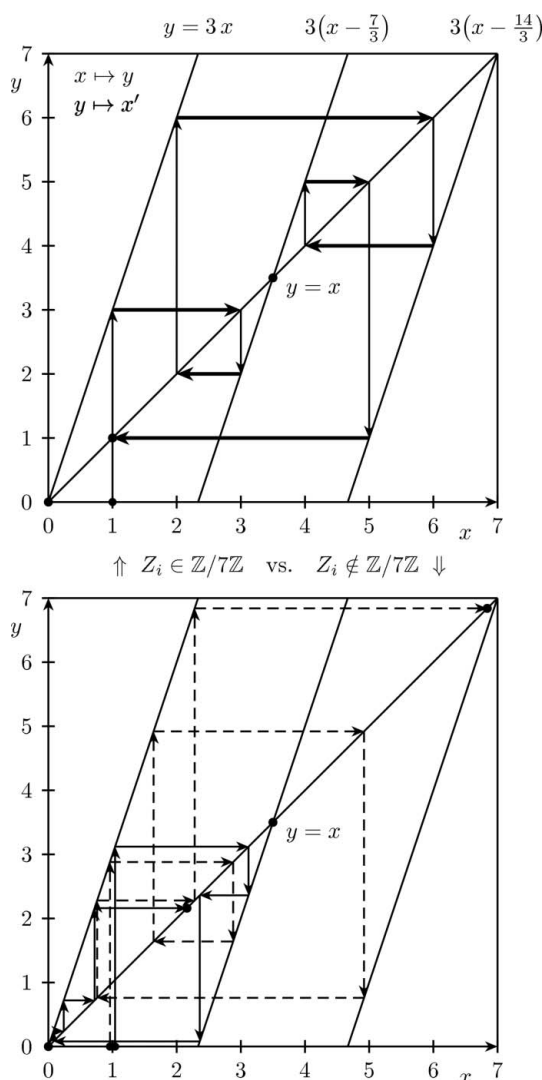


Figure 7

Top: iterative mapping related to the MCG with $m = 3$ and $M = 7$ and integer seed value $Z_1 = 1$. The mapping can be conceived as consisting of alternating steps, the first one, $x \rightarrow y$ (thin lines), describing the action of the MCG ($x = Z_n, y = Z_{n+1}$) and a second one, $y \rightarrow x'$ (thick lines), due to the recursive nature of the discrete dynamical process. Emphasized are the fixpoints (0) and (3.5) and the period-six orbit (132645). Bottom: iterative mappings related to the MCG with $m = 3$ and $M = 7$ and rational seed values of $Z_1 = 0.96$ (dashed line) and $Z_1 = 1.04$ (solid line). The corresponding orbits are periodic but with period 60 rather than six, because $3^{60}0.96 \equiv 0.96 \pmod{7}$. In fact, both starting values describe the same orbit, since $3^{10}0.96 \equiv 1.04 \pmod{7}$. Nevertheless, starting from distinct points and examining the trajectories after a limited number of steps (here six, as compared to the orbit with starting value $Z_1 = 1$) shows a strong divergence of intermediate values in contrast to the nearby located seed values.

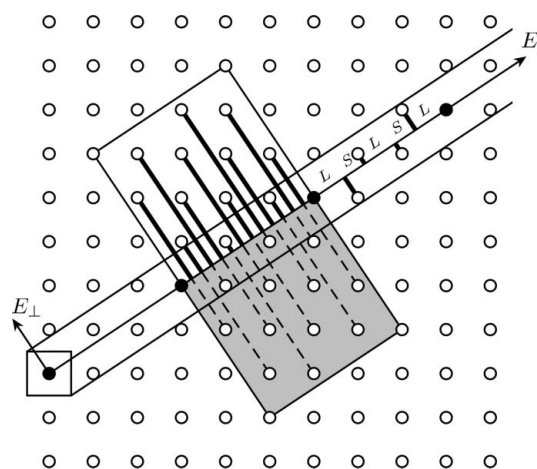


Figure 8

Relation of a Fibonacci chain quasicrystal approximant with a sequence $(LSLSL)_{\infty}$ of short and long distances to (i) a similar sublattice of index 13 with square symmetry, and (ii) an MCG with $\mu = 8$ and $M = 13$. Shown are the directions of the parallel and perpendicular Euclidean subspaces for the description of a one-dimensional, codimension-one quasicrystal and its approximants. The projection window is defined by the unit cell of the basic lattice, whereas sites of different conumbering [0, 13] are situated inside the unit cell of the sublattice. Note that the sum of orthogonal distances, adding up bold and dashed lines for a given site of E_{\parallel} and along opposite directions of E_{\perp} , is always equal to a sublattice translation. Two sites of the same conumbering define the translation period within the physical space E_{\parallel} (conventionally the ones with a conumbering of zero, represented here with filled circles, are chosen as the origin and its translates).

It is a pleasure to thank Robert Grzimek for his enlightening remarks on the manuscript, which helped to improve it. Furthermore, I am indebted to Sven Lidin and Juan Manuel Pèrez-Mato for both granting me access to some of their research results prior to publication. Dieter Herlach's and my colleagues' endorsement at DLR, Cologne is kindly acknowledged.

References

- Alligood, K. T., Sauer, T. D. & Yorke, J. A. (1996). *Chaos – an Introduction to Dynamical Systems*, 2nd ed. New York, Berlin, Heidelberg: Springer.
- Baake, M., Scharlau, R. & Zeiner, P. (2011). *Can. J. Math.* **63**, 1220–1237.
- Brenner, J. L. (1973). *Pacific J. Math.* **45**, 413–414.
- Burzlaff, H. & Malinovsky, Y. (1997). *Acta Cryst.* **A53**, 217–224.
- Burzlaff, H. & Rothammel, W. (1992). *Acta Cryst.* **A48**, 483–490.
- Coxeter, H. S. M. (1948). *Reports of a Mathematical Colloquium*, 2nd series, Vol. 8, pp. 18–38.
- Dorst, L., Fontijn, D. & Mann, S. (2007). *Geometric Algebra for Computer Science – an Object-oriented Approach to Geometry*, 1st ed. San Francisco: Morgan Kaufmann Publishers.
- Duneau, M., Mosseri, R. & Oguey, C. (1989). *J. Phys. A Math. Gen.* **22**, 4549–4564.
- Elenius, M., Zetterling, F. H. M., Dzugutov, M., Fredrickson, D. C. & Lidin, S. (2009). *Phys. Rev. B*, **79**, 144201.
- Eon, J.-G. (2011). *Acta Cryst.* **A67**, 68–86.
- Figueiredo, M. O. (1973). *Acta Cryst.* **A29**, 234–243.
- González, S., Pèrez-Mato, J. M., Elcoro, L. & García, A. (2011). *Phys. Rev. B*, **84**, 184106.
- Gugisch, R., Kerber, A., Laue, R., Meringer, M. & Rücker, C. (2007). *MATCH Commun. Math. Comput. Chem.* **58**, 239–280.
- Hardy, G. H. & Wright, E. M. (2008). *An Introduction to the Theory of Numbers*, 6th ed. Oxford, New York: Oxford University Press.
- Herring, C. & Palmore, J. I. (1989). *ACM SIGPLAN Not.* **24**, 76–79.
- Hoch, C. (2010). Personal communication.
- Hoppe, R. (1998). *Z. Anorg. Allg. Chem.* **624**, 1877–1885.
- Hoppe, R. (2004). *Z. Anorg. Allg. Chem.* **630**, 2384–2392.
- Hornfeck, W. (2010). PhD thesis, Philipps-University, Marburg, Germany. <http://archiv.ub.uni-marburg.de/diss/z2010/0560/>.
- Hornfeck, W. & Harbrecht, B. (2009). *Acta Cryst.* **A65**, 532–542.
- Hyslop, J. (2008). *Crystal Lattice Models, Explore Whipple Collections*, Whipple Museum of the History of Science, University of Cambridge. <http://www.hps.cam.ac.uk/whipple/explore/models/modellingchemistry/crystallatticemodels/>.
- Iida, S. (1957). *J. Phys. Soc. Jpn.* **12**, 222–233.
- Janner, A. (2004). *Acta Cryst.* **A60**, 611–620.
- Katsura, S. & Fukuda, W. (1985). *Physica A*, **130**, 597–605.
- Kerber, A., Laue, R., Meringer, M. & Rücker, C. (2004). *J. Comput. Chem. Jpn.* **3**, 85–96.
- Konno, H. & Kondo, T. (1997). *Ann. Nucl. Energy*, **24**, 1183–1188.
- Lemke, P., Skiena, S. S. & Smith, W. D. (2002). *Reconstructing Sets from Interpoint Distances*. DIMACS Technical Report 2002–37. Rutgers University, Piscataway, NJ, USA.
- Lima-de-Faria, J. (1978). *Z. Kristallogr.* **148**, 1–5.
- Lima-de-Faria, J. (1983). *Acta Cryst.* **B39**, 317–323.
- Loeb, A. L. (1964). *Acta Cryst.* **17**, 179–182.
- Loeb, A. L. (1990). *Per. Mineral.* **59**, 197–217.
- Mackay, A. L. (1984). *Croat. Chem. Acta*, **57**, 725–736.
- May, R. M. (1976). *Nature (London)*, **261**, 459–467.
- Mosseri, R. (1988). *Universalities in Condensed Matter (Springer Proc. Phys.)*, edited by R. Jullien, L. Peliti, R. Ramma & N. Boccara, Vol. 32, pp. 9–14. Berlin, Heidelberg: Springer.
- Nyman, H., Carroll, C. E. & Hyde, B. G. (1991). *Z. Kristallogr.* **196**, 39–46.
- O'Keeffe, M. (1992). *Acta Cryst.* **A48**, 879–884.
- O'Keeffe, M. & Andersson, S. (1977). *Acta Cryst.* **A33**, 914–923.
- Palmore, J. & Herring, C. (1990). *Physica D*, **42**, 99–110.
- Patterson, A. L. (1944). *Phys. Rev.* **65**, 195–201.
- Pearson, W. B. (1972). *The Crystal Chemistry and Physics of Metals and Alloys*, 1st ed. New York: Wiley-Interscience.
- Sadoc, J.-F. & Mosseri, R. (1999). *Geometrical Frustration*, 1st ed. Cambridge, New York: Cambridge University Press.
- Spek, A. L. (2009). *Acta Cryst.* **D65**, 148–155.
- Takeda, H. & Donnay, J. D. H. (1965). *Acta Cryst.* **19**, 474–476.
- Vidal, J. & Mosseri, R. (2000). *Mater. Sci. Eng.* **294–296**, 572–575.
- Villars, P. & Cenzual, K. (2007). *Pearson's Crystal Data: Crystal Structure Database for Inorganic Compounds (on CD-ROM)*, Version 1.0, Release 2007/8, ASM International, Materials Park, OH, USA.
- Weininger, D. (1988). *J. Chem. Inf. Comput. Sci.* **28**, 31–36.
- Wiener, H. (1947). *J. Am. Chem. Soc.* **69**, 17–20.
- Wintgen, G. (1941). *Math. Ann.* **118**, 195–215.
- Wiswesser, W. J. (1985). *J. Chem. Inf. Comput. Sci.* **25**, 258–263.
- Wolfram, S. (2002). *A New Kind of Science*, 1st ed. Champaign: Wolfram Media, Inc.
- Zobetz, E. (1993). *Z. Kristallogr.* **207**, 209–222.